HHS Public Access

Author manuscript

Dalton Trans. Author manuscript; available in PMC 2016 August 31.

Published in final edited form as:

Dalton Trans. 2012 June 7; 41(21): 6558–6566. doi:10.1039/c2dt12207c.

Exploring the Reactivity of Flavonoid Compounds with Metal-Associated Amyloid-β Species

Xiaoming He[a], **Hyun Min Park**[a,b], **Suk-Joon Hyung**[c], **Alaina S. DeToma**[c], **Cheal Kim**[b], **Brandon T. Ruotolo**[c], and **Mi Hee Lim**[a,c,*]

[a]Life Sciences Institute, University of Michigan, Ann Arbor, MI 48109-2216 (USA)

[b]Department of Chemistry, Seoul National University of Science and Technology, Seoul 139-743 (Korea)

[c]Department of Chemistry, University of Michigan, Ann Arbor, MI 48109-1055 (USA)

Abstract

Metal ions associated with amyloid-β (Aβ) peptides have been suggested to be involved in the development of Alzheimer's disease (AD), but this remains unclear and controversial. Some attempts to rationally design or select small molecules with structural moieties for metal chelation and Aβ interaction (*i.e.*, bifunctionality) have been made to gain a better understanding of the hypothesis. In order to contribute to these efforts, four synthetic flavonoid derivatives **FL1** – **FL4** were rationally selected according to the principles of bifunctionality and their abilities to chelate metal ions, interact with Aβ, inhibit metal-induced Aβ aggregation, scavenge radicals, and regulate the formation of reactive oxygen species (ROS) were studied using physical methods and biological assays. The compounds **FL1** – **FL3** were able to chelate metal ions, but showed limited solubility in aqueous buffered solutions. In the case of **FL4**, which was most compatible with aqueous conditions, its binding affinities for Cu^{2+} and Zn^{2+} (nM and μM, respectively) were obtained through solution speciation studies. The direct interaction between **FL4** and Aβ monomer was weak, which was monitored by NMR spectroscopy and mass spectrometry. Employing **FL1** – **FL4**, no noticeable inhibitory effect on metal-mediated Aβ aggregation was observed. Among **FL1** – **FL4**, **FL3**, having 3-OH, 4-oxo, and 4′-$N(CH_3)_2$ groups, exhibited similar antioxidant activity to the vitamin E analogue, Trolox, and *ca.* 60% reduction in the amount of hydrogen peroxide (H_2O_2) generated by Cu^{2+}-Aβ in the presence of dioxygen (O_2) and a reducing agent. Overall, the studies here suggest that although four flavonoid molecules were selected based on expected bifunctionality, their properties and metal-Aβ reactivity were varied depending on the structure differences, demonstrating that bifunctionality must be well tuned to afford desirable reactivity.

Introduction

Alzheimer's disease (AD) is the most common form of dementia in the elderly population that is characterized by memory loss, language impairment, personality changes, and decline in intellectual ability.[1–3] The accumulation of amyloid-β (Aβ) peptides and high levels of

*To whom correspondence should be addressed: mhlim@umich.edu.

oxidative stress are two pathological features of AD.[1–5] The molecular mechanisms of AD, however, are highly complex and still elusive. In the past two decades, the role of essential metal ions in AD has aroused great interest.[1–4,6–14] Elevated concentrations of metal ions, such as Cu, Zn, and Fe, were found to be associated with Aβ plaques in the diseased brain suggesting that their possible interaction could contribute to pathological events in AD (*e.g.,* Aβ aggregation, reactive oxygen species (ROS) production). Metal chelating agents, such as clioquinol (Fig. 1) and PBT2, have been shown to interrupt metal-Aβ interaction and reduce neurotoxicity, and subsequently, they have been proposed as a potential therapeutic approach for AD.[1–4,13–19]

To gain a better understanding of the role of metal ions in AD and the relationship between metal-Aβ interaction/reactivity and AD pathology, multifunctional metal chelators have been developed.[2,4,14,19] Most of the recent attention has been focused on a rational structure-based design strategy that grants bifunctionality (metal chelation and Aβ interaction) *via* inclusion of suitable structural moieties within one molecule. Previously reported bifunctional molecules by our group and others have been constructed utilizing known Aβ interacting frameworks, including thioflavin-T (ThT) (Fig. 1), (*E*)-4-iodo-4′-dimethylamino-1,2-diphenylethylene (*p*-I-stilbene), and 4-(7-iodoimidazo[1,2-*a*]pyridin-2-yl)-*N*,*N*-dimethylaniline (IMPY).[4,14,19–29] Compared to traditional metal chelators that do not have the Aβ interacting structures, these bifunctional compounds may be valuable in specifically targeting metal-Aβ species and investigating their related events.

Currently, the development of bifunctional small molecules for targeting and controlling metal-Aβ species is in incipient stages. Searching for a new class of structural frameworks that can provide appropriate bifunctionality to target metal-Aβ species and control their interaction/reactivity is still crucial toward the design of chemical tools. Naturally occurring polyphenolic compounds, such as flavonoids, have presented broad biological and pharmacological activities.[30,31] Some of the flavonoids have the potential advantages of being antioxidants and being able to interact with Aβ species and/or metal ions.[28,30–38] Some synthetic flavonoid derivatives have also been used as Aβ plaque imaging agents.[37,38] These properties render flavonoids as valuable candidates for chemical tools to possibly interact with metal-Aβ species, and this reactivity was recently demonstrated for one of the natural flavonoid compounds, myricetin (Fig. 1).[28] Myricetin was capable of modulating metal-induced Aβ aggregation *in vitro* and attenuating metal-Aβ toxicity in living cells, supporting the exploration of the core flavonoid framework as a template for the design and/or selection of bifunctional molecules for metal-Aβ species.

To further pursue the development of multifunctional small molecules for targeting and modulating metal-Aβ species, four flavonoid compounds (**FL1** – **FL4**, Fig. 1) were selected, prepared, and studied. These molecules were rationally chosen according to elements of the incorporation design strategy and were expected to have potential functions for metal binding, Aβ interaction, and antioxidant ability.[28,30–38] In order to understand the structural elements that facilitate the interaction and reactivity between flavonoid derivatives and metal-Aβ species, the structures **FL1** – **FL4** have been simplified compared to myricetin to contain one or two potential metal chelation sites. In addition, a dimethylamino group was taken into account in the structures of **FL2** and **FL3** similarly to flavonoid-based imaging

agents.[25,27,37–39] Studies of these structures with Aβ or metal-Aβ species could present insight into how variations of the chemical structures of flavonoids may be useful in order to contribute to the discovery of suitable chemical tools for investigating metal-Aβ species in AD. Herein, our investigations of four flavonoid compounds' properties (*e.g.*, metal chelation, Aβ interaction, antioxidant ability) and reactivity toward metal-Aβ species, including the ability to regulate metal-mediated Aβ aggregation and ROS production, are described.

Experimental

Materials and methods

All chemical reagents and solvents were purchased from commercial suppliers and used as received unless otherwise specified. 5-Hydroxyflavone (**FL1**),[40] 5-hydroxy-4′-dimethylaminoflavone (**FL2**),[40] 3-hydroxy-4′-dimethylaminoflavone (**FL3**),[41,42] and 3-hydroxy-2-(pyridin-2-yl)-4H-chromen-4-one (**FL4**)[42] were prepared following previously reported procedures. $A\beta_{1\text{-}40}$ peptide (free acid terminal) was purchased from AnaSpec (> 95% purity, Fremont, CA, USA). For the NMR investigations, ^{15}N-labeled $A\beta_{1\text{-}40}$ was purchased from rPeptide (Athens, GA, USA). The amino acid sequence for the $A\beta_{1\text{-}40}$ peptide is DAEFRHDSGYEVHHQKLVFFAEDVGSNKGAIIGLMVGGVV. The horseradish peroxidase (HRP)/Amplex Red assay to measure hydrogen peroxide (H_2O_2) production was performed according to previous reports.[24,25,27,43,44] The studies of investigating the effect of compounds on Aβ aggregation were conducted according to the previously reported protocols.[24–28]

^{1}H NMR (400 MHz) and ^{13}C NMR (100 MHz) spectra, with chemical shifts relative to tetramethylsilane (TMS) or to solvent residual peaks as the internal standard, were recorded on a 400 MHz Varian NMR spectrometer. Mass spectrometric measurements of the ligands were performed using a Micromass LCT Electrospray Time-of-Flight mass spectrometer. The NMR investigation of the interaction of **FL4** with Aβ was conducted using a 900 MHz Bruker Avance spectrometer (Michigan State University, East Lansing, MI, USA). Mass spectra for studying the interaction of Aβ with compounds were acquired on an LCT Premier mass spectrometer (Waters, Milford, MA, USA) fitted with a nano-electrospray ionization (nESI) source. UV-Visible (UV-Vis) spectra were recorded on an Agilent 8453 UV-Vis spectrophotometer. Fluorescence spectra were measured on a FluoroMax-3 spectrophotometer. A SpectraMax M5 microplate reader (Molecular Devices, Sunnyvale, CA, USA) was used for measurements of absorbance and fluorescence for the Trolox equivalent antioxidant capacity (TEAC) assay and the HRP/Amplex Red assay, respectively.

3-Hydroxy-4′-dimethylaminoflavone (FL3)—FL3 was synthesized according to the previously reported procedures.[41,42] ^{1}H NMR (400 MHz, CD_2Cl_2) /δ (ppm): 8.18 (m, 3 H), 7.68 (t, J = 7.6 Hz, 1 H), 7.59 (d, J = 8.4 Hz, 1 H), 7.39 (t, J = 7.4 Hz, 1 H), 6.95 (s, 1 H), 6.81 (d, J = 9.2 Hz, 2 H), 3.06 (s, 6 H). ^{13}C NMR (100 MHz, CD_2Cl_2) /δ (ppm): 172.3, 155.1, 151.4, 146.3, 136.8, 132.8, 129.0, 124.9, 124.1, 120.8, 118.0, 117.9, 111.3, 39.8. HRMS (*m/z*) (ESI+): Calcd for $C_{17}H_{16}NO_3$ ([M+H]$^+$), 282.1130; Found, 282.1124.

Metal binding studies

The metal binding studies of **FL4** in the absence and presence of Aβ were investigated using UV-Vis and emission spectroscopy in a buffered solution (20 mM 2-[4-(2-hydroxyethyl)-piperazin-1-yl]ethanesulfonic acid (HEPES), pH 7.4, 150 mM NaCl). Due to the limited solubility of **FL1** – **FL3** in aqueous media, their metal binding studies were carried out in EtOH. Acidity constants (pK_a) of **FL4** and the stability constants (log β) of its corresponding metal complexes were determined by UV-Vis variable-pH titrations according to the reported procedures.[25–27] To measure the pK_a values for the ligand, a solution of **FL4** (50 μM in 100 mM NaCl, 10 mM NaOH, pH 12) was titrated with small aliquots of HCl. At least 30 spectra were obtained in the range from pH 2.0 – 12. Similarly, to obtain the stability constants (log β) of the metal-ligand complexes, a solution containing **FL4** (50 μM or 100 μM) and a metal chloride salt in a metal/ligand ratio of 1:2 ($[CuCl_2]$ = 25 μM; $[ZnCl_2]$ = 50 μM) was titrated with small additions of HCl over the range of pH 2.0 – 8.0 (at least 30 spectra). The acidity and stability constants were calculated using the HypSpec program (Protonic Software, UK).[45] The speciation diagrams of **FL4** and its corresponding metal complexes were modeled using the program HySS2009 (Protonic Software).[46]

Two-dimensional (2D) ^1H–^{15}N transverse relaxation optimized spectroscopy (TROSY)-heteronuclear single quantum correlation (HSQC) NMR measurements

^{15}N-labeled $A\beta_{1\text{-}140}$ (*ca.* 0.25 mg) was dissolved into 186 μL of a buffer solution containing sodium dodecyl-d_{25} sulfate (SDS-d_{25}, 200 mM), sodium phosphate buffer (20 mM, pH 7.3), and D_2O (7%, v/v), and briefly vortexed. The peptide solution (*ca.* 308 μM) was transferred to a Shigemi NMR tube. After acquiring spectra of the peptide, 20 equivalents of **FL4** (stock solution: 5 mM in the NMR buffer solution) were added to the Aβ sample. Due to the solubility limitation, NMR experiments with **FL1** – **FL3** were not carried out. 2D ^1H–^{15}N TROSY–HSQC NMR measurements were recorded on the 900 MHz Bruker Avance NMR spectrometer (equipped with a TCI cryoprobe accessory) with 14.3 kHz and 1.7 kHz spectral width and 2048 and 128 complex data points in the ^1H and ^{15}N dimensions, respectively, 4 scans for each t_1 experiment, and 1.5 s recycle delay; each spectrum took 10 min for completion.[24–27] Water peak was referenced to 4.78 ppm at 25 °C. ^1H–^{15}N HSQC peaks were assigned by comparison of the observed chemical shift values with those reported in the literature.[47] Combined ^1H and ^{15}N 2D chemicals shifts ($\Delta\delta_{N-H}$) were calculated from equation (1).[48–50] The 2D results were processed using Topspin software (version 2.1 from Bruker) and analyzed with Sparky (version 3.112).

$$\Delta\delta_{N-H} = \sqrt{\frac{(\Delta\delta_H)^2 + (0.2(\Delta\delta_N))^2}{2}} \quad (1)$$

Mass spectrometric measurements

Samples were prepared by mixing stock solutions of **FL4** (1% v/v DMSO) and $A\beta_{1\text{-}40}$ (dissolved in the aqueous solvent containing 100 mM ammonium acetate at pH 7.0) to generate a final peptide concentration of 10 μM. To generate protein complex ions, an

aliquot of the sample (*ca.* 5 μL) was sprayed from the nESI emitter using capillary voltages ranging from 1.8 – 2.0 kV, with the source operating in positive ion mode and the sample cone operated at 20 V. The mass spectra were acquired with the following settings and tuned to avoid ion activation and preserve non-covalent protein-ligand complexes: ion guide, 20 V; ion energy, 100 V; ToF analyzer pressure, 3.01 x 10^{-6} mbar; and N_2 was used as the desolvation gas.

Trolox equivalent antioxidant capacity (TEAC) assay

The TEAC assay is used to determine the antioxidant ability based on the extent of decolorization of ABTS (2,2′-azino-bis(3-ethylbenzothiazoline-6-sulfonic acid) diammonium salt) cation radical relative to that of the vitamin E analogue, Trolox.[51] The assay was performed according to the previously reported method with slight modifications.[51,52] First, blue $ABTS^{\cdot+}$ cation radicals were generated by dissolving ABTS (19 mg, 7.0 mM) with potassium persulfate (3.3 mg, 2.5 mM) in 5 mL water and incubating for 16 h at room temperature in the dark. The resulting $ABTS^{+\cdot}$ solution was diluted with EtOH to an absorbance of *ca.* 0.7 at 734 nm. The assay was conducted in a clear 96 well plate to which 200 μL diluted $ABTS^{+\cdot}$ solution was added and incubated at 30 °C for 5 min in the plate reader. Each ligand was added from a stock solution prepared in DMSO (final, 1% v/v) or in EtOH (for Trolox) and was incubated with the $ABTS^{+\cdot}$ solution at 30 °C for different time periods (1, 3, 6, 10, 15, and 30 min). The percent inhibition was calculated according to the measured absorbance at 734 nm (% Inhibition = 100 × $(A_0 – A)/A_0$) and was plotted as a function of ligand concentration. The TEAC value of compounds for each time point was calculated as a ratio of the slope of the standard curve of the compound to that of Trolox. The measurements were carried out in triplicate.

Horseradish Peroxidase (HRP)/Amplex Red assay

The production of H_2O_2 generated by Cu^{2+}-Aβ species in the presence of dioxygen (O_2) and a reducing agent (ascorbate) was measured using the modified horseradish peroxidase (HRP)/Amplex Red assay.[24,25,27,43,44] The assay was performed *in situ* and carried out in black polystyrene 96 well plates. In each well, fresh $Aβ_{1-40}$ (200 nM) in phosphate buffered saline (PBS, pH 7.4) was treated with $CuCl_2$ (400 nM) and was incubated for 1 h at room temperature with constant agitation. Each ligand (800 nM, 1% v/v DMSO) was introduced to the resulting solution followed by additional incubation at room temperature with constant agitation. After 1 h, the solution of ascorbate (10 μM) was added into each well. After 5 min treatment, the reaction solution containing Amplex Red (50 μM) and HRP (1 U/mL) was treated to individual samples. After 15 min incubation, the fluorescence emission intensity was measured ($\lambda_{ex/em}$ = 530/590 nm) using a microplate reader. Catalase (10 μL of 100 U/mL) was used for the samples to confirm H_2O_2 production in the system. The total volume was 100 μL in each well.

Amyloid-β (Aβ) Peptide Experiments

The $Aβ_{1-40}$ samples were prepared according to the previously reported procedures.[24–28] The Aβ peptide was dissolved in NH_4OH (1% w/v, aq), lyophilized, and stored at –80 °C. Stock solutions of Aβ were prepared prior to the experiments by redissolving the lyophilized Aβ with NH_4OH (1% v/v, aq, 10 μL) and diluting with ddH_2O. All solutions for inhibition

and disaggregation studies were prepared in a buffered solution (20 μM HEPES, pH 6.6 or 7.4, 150 μM NaCl). For the inhibition studies, fresh Aβ (10 μM) was incubated with either $CuCl_2$ or $ZnCl_2$ (10 μM) for 2 min at room temperature followed by addition of **FL1** – **FL4** (20 μM). The solutions were incubated for 24 h at 37 °C with constant agitation. For the disaggregation studies, Aβ aggregates were prepared by treating fresh Aβ (25 μM) with $CuCl_2$ or $ZnCl_2$ (25 μM) and incubating for 24 h at 37 °C with constant agitation. Afterwards, **FL4** (50 μM) was added and the resulting solutions were incubated for 24 h at 37 °C with continuous agitation. Metal-free Aβ samples were prepared at the same condition in the absence of metal chloride salts. The resulting Aβ species were analyzed using native gel electrophoresis using Western blotting with an anti-Aβ antibody 6E10.[24–28] Each sample (10 μL) was separated on a 10 – 20% gradient Tris-tricine gel (Invitrogen). The gel was transferred onto a nitrocellulose membrane, blocked with bovine serum albumin (BSA, 3% w/v, Sigma) in Tris-buffered saline (TBS, Fisher) containing 0.1% Tween-20 (TBS-T, Sigma) overnight at room temperature, and incubated with an anti-Aβ antibody 6E10 (1:2,000) in 2% BSA in TBS-T for 4 h at room temperature. The membrane was probed with the HRP-conjugated goat anti-mouse antibody (1:5,000) in 2% BSA in TBS-T for 1 h at room temperature. The Thermo Scientific Supersignal West Pico Chemiluminescent Substrate was used to visualize protein bands.

Results and discussion

Selection and preparation

Continued exploration of a new class of structural frameworks that have bifunctionality is necessary in order to optimize aspects of their reactivity, including metal-Aβ aggregation regulation, antioxidant capacity, or blood-brain barrier (BBB) permeability, as compared with previously reported bifunctional compounds.[2,4,14,20–27,29] Naturally occurring flavonoids have exhibited antioxidative, metal binding, and antiamyloidogenic properties, making them promising candidates for the development of multifunctional small molecules for targeting and modulating metal-Aβ species in AD.[28,30–38] Recently, we demonstrated that the flavonoid compound, myricetin, could mediate metal-induced Aβ aggregation *in vitro* and reduce metal-Aβ neurotoxicity in living cells.[28] In an effort to ascertain how structural modifications of this framework would impact reactivity, four flavonoid compounds (**FL1** – **FL4**, Fig. 1) were rationally selected based on their direct inclusion of a metal binding site into the Aβ interacting scaffold (incorporation approach of rational structure-based design strategy)[2,4,14,19] and prepared following the previously reported methods.[40–42] These compounds **FL1** – **FL4** additionally satisfy the restrictive terms of Lipinski's rules and the range of the desired calculated logBB value (Table S1), which suggests their potential brain uptake.[53,54] Structurally, the metal binding sites are located at 4-oxo and 5-OH or 3-OH groups of **FL1**, **FL2**, and **FL3**, two of the probable binding sites in natural flavonoids. In addition to that, for **FL4**, a 2-pyridinyl N donor atom was introduced into the flavonoid framework to provide an additional metal binding site along with either the 3-OH or the O donor atom of the benzopyran ring.[42] This heteroatom incorporation into the structure also provides enhancement to solubility in aqueous conditions that is a limitation for **FL1** – **FL3.** Furthermore, **FL2** and **FL3** contain a dimethylamino group, which has been suggested to be a critical structural moiety for Aβ interaction.[25,27,37–39]

Metal binding properties

The metal chelation abilities of **FL1** – **FL4** were studied using UV-Vis and emission spectroscopy (Figs. 2 and S1). As shown in Fig. S1, the optical spectrum of **FL1** in EtOH exhibited absorption bands at 270 nm (with a shoulder at 295 nm) and 336 nm. Introduction of a dimethylamino group ($N(CH_3)_2$) in the flavonoid scaffold led to red-shifted absorption bands at 390 and 402 nm for **FL2** and **FL3**, respectively, relative to those for **FL1**. Incubation of **FL1** – **FL3** with 1 equivalent of $CuCl_2$ in EtOH induced optical band shifts showing new bands at *ca.* 415 and 468 nm for **FL1** and **FL3**, respectively, and small optical band shift for **FL2**. Upon treatment with 1 equivalent of $ZnCl_2$ **FL3** produced a noticeable spectral change, while no significant optical shifts were observed when **FL1** or **FL2** was treated with $ZnCl_2$ (even with an excess of $ZnCl_2$). The observable optical change of **FL3** incubated with $ZnCl_2$ may be due to the stronger acidity of the 3-OH group over the 5-OH group, which would enhance metal chelation by **FL3**.[36]

Compared to **FL1** – **FL3**, **FL4** is relatively soluble in aqueous media. In the buffer solution (20 mM HEPES, pH 7.4, 150 mM NaCl), **FL4** presented intense absorption bands at 240, 256, 318, and 354 nm and an emission band at 534 nm (λ_{ex} = 383 nm) (Fig. 2). Upon addition of $CuCl_2$ or $ZnCl_2$, new absorption bands at *ca.* 400 – 500 nm were formed showing three isosbestic points (267, 298, and 383 nm for Cu^{2+} binding; 268, 290 and 383 nm for Zn^{2+} binding). In the case of emission studies, *ca.* 80% and 95% quenching in emission upon addition of 0.5 and 1 equivalent of $CuCl_2$ to the solution of **FL4** was observed, respectively (Fig. 2). On the contrary, an increase in emission with a modest hypsochromic shift occurred when **FL4** was incubated with $ZnCl_2$. The emission of **FL4** with 0.5 and 1 equivalent of Zn^{2+} was enhanced by 2.4(±0.3)-fold and 3.4(±0.1)-fold, respectively. Based on the previous photophysical studies of **FL4**, two conformers could exist in equilibrium in solution *via* the formation of different hydrogen bonding interactions between either the 3-OH and 4-oxo groups or the 3-OH group and the pyridyl N donor atom.[42] Both conformers could undergo the excited-state intramolecular proton transfer (ESIPT) reaction upon excitation affording their different emission behaviors. Zn^{2+} binding of **FL4** may contribute to the inhibition of the equilibrium between two conformers and/or the photoinduced electron transfer (PET) process, which would enhance emission intensity of the ligand.

To further understand the solution speciation of **FL4** and its corresponding metal complexes, UV-Vis variable-pH titration experiments were performed following the previously reported method (Figs. 3, 4, and S2).[25–27] Spectrophotometric titrations of **FL4** from a range of pH 2.0 to 12 were first carried out at room temperature (I = 0.10 M NaCl) to determine its acidity constants (K_a) (Figs. 3 and S2). Two pK_a values for **FL4** (pK_{a1} = 2.011(8); pK_{a2} = 9.3892(3)) were obtained. Using these acidity constants, a solution speciation diagram (Fig. 3) was calculated suggesting that the neutral molecule **FL4** is the predominant species (*ca.* 99%) at pH 7.4. Solution speciation studies of Cu^{2+} or Zn^{2+} complexes of **FL4** were also conducted under the same condition (1:2 [M]/[**FL4**], I = 0.10 M NaCl, room temperature) by UV-Vis variable-pH titrations and their stability constants (log β) were calculated (pK_a values of **FL4** and hydrolysis of free metal ions were considered in the calculations) (Figs. 4 and S2). On the basis of the stability constants, speciation diagrams were calculated for Cu^{2+} and Zn^{2+} with **FL4** (Fig. 4). These diagrams suggest that a mixture of 1:1 and 1:2 metal

complexes of **FL4** with Cu^{2+} or Zn^{2+} exist at pH 7.4. In addition, the concentration of free Cu^{2+} above pH 5.0 with the ligand was negligible, while free Zn^{2+} was present up to pH 8.0. From these solution speciation diagrams, the concentrations of unchelated Cu^{2+} and Zn^{2+} ($pM = -\log[M_{unchelated}]$) at a specific pH value can be calculated to represent the metal binding affinity of the ligand (pCu = 8.0 and 8.9 at pH 6.6 and pH 7.4, respectively; pZn = 6.5 at pH 7.4). These pM values, corresponding to the approximate dissociation constant (K_d), indicate that the K_d values of **FL4** are comparable to those of Cu-Aβ (picomolar to nanomolar) and Zn-Aβ (micromolar).[2–4,8,9,25] Thus, the affinities of **FL4** for Cu^{2+} and Zn^{2+} suggest that this ligand might be able to compete with Aβ for metal binding.

Interaction with Aβ monomer

Along with the metal binding properties, Aβ interaction of the ligand (**FL4**) in the absence of metal ions was explored using NMR and MS techniques. First, high-resolution 2D TROSY–HSQC NMR spectroscopy was employed using ^{15}N-labeled $Aβ_{1-40}$ in the presence of SDS micelles. Under such conditions, the Aβ peptide maintains the monomeric form and adopts an α-helical conformation in the region of Q15 – V36,[47,55] which may be related to the early stages in the formation of Aβ aggregated species. Modest changes in chemical shifts were observed upon addition of 20 equivalents of **FL4** to the solution containing Aβ (308 μM, 200 mM SDS-d_{25}, 20 mM sodium phosphate, 7% D_2O (v/v), pH 7.3, Fig. 5). **FL4** exerted an influence on residues of E11 and H13, which are close to the metal binding site (H6, H13, and H14) in Aβ.[1–4,8–14] Potentially, this may allow the molecule to chelate metal ions from metal-bound Aβ species. These NMR data, however, imply that **FL4** is weakly interacting with Aβ monomer as compared with our previously reported bifunctional small molecules.[24–27] Even with the higher concentration of **FL4**, the degree of Aβ interaction is similar to that of a traditional metal chelator, 8-hydroxyquinoline (8-HQ), which lacks specific structural components for Aβ interaction.[25] This observation was also confirmed by the mass spectrometric investigation of **FL4** with Aβ monomer in an SDS-free condition. With a five-fold excess of **FL4**, no clear evidence of binding to monomeric Aβ species was indicated (Fig. S3). Taken together, the weak interaction between monomeric Aβ and **FL4** was suggested by NMR and MS studies and may propose that additional structural moieties would be necessary for interaction with Aβ monomer.

Antioxidant ability

The antioxidant ability of flavonoids is one of their important biological activities that has been studied and reviewed, with radical scavenging as a widely accepted mechanism.[30,31,56] To verify the antioxidant activity of compounds **FL1** – **FL4**, the Trolox equivalent antioxidant capacity (TEAC) assay was employed.[51,52] As shown in Fig. 6, only **FL3** displayed noticeable ability to quench the radical; its activity was comparable to that of the vitamin E analogue, Trolox, but less than that of myricetin.[56] Although all of these molecules contain the 2,3-double bond and 4-oxo group, which has been shown to be beneficial for imparting antioxidant activity in flavonoids, possible intramolecular hydrogen bonding may impede their ability to serve as a H donor to the radical.[56] In particular, in the case of **FL4**, the intramolecular hydrogen bonding interaction of the 3-OH group with the 4-oxo group or the pyridyl N donor atom has been demonstrated and could be a factor in the

lower antioxidant activity.[42] Compared to **FL1**, **FL2**, and **FL4**, the higher antioxidant activity of **FL3** and myricetin suggests that appropriate placement of the OH and oxo groups, along with other functionalities (*e.g.*, dimethylamino and/or OH groups) may help convey antioxidant activity.

Influence on metal-induced Aβ events

Based on the metal binding affinities of **FL4** (*vide supra*), it is possible that this ligand could sequester Cu^{2+} or Zn^{2+} from soluble Aβ species.[2–4,8,9,25] In order to examine this, optical and emission studies of **FL4** with metal-treated Aβ species were conducted (Fig. 7; [Aβ] = 25 μM, [M^{2+}] = 25 μM, [**FL4**] = 50 μM). Distinct optical and emission spectral responses were observed from the samples containing **FL4**, Aβ, and metal ions, similar to the spectral changes in the metal binding studies of the ligand in Aβ-free solution. In the case of the sample containing Aβ, Cu^{2+}, and **FL4** (1:1:2 ratio), 60(±6)% quenching in emission of the ligand was observed relative to that of Aβ and **FL4** (1:2 ratio) (Fig. 7c). As shown in Fig. 2, the sample of Cu^{2+} and **FL4** in a 1:2 ratio in the absence of Aβ exhibited 80(±2)% quenching in emission, compared to the emission intensity of **FL4** only. Upon treatment of 2 equivalents of **FL4** into the sample of Aβ and Zn^{2+}, the emission intensity was increased by 2.4(±0.3)-fold, compared to that from the solution of Aβ and **FL4** (Fig. 7d). Chelation of Zn^{2+} by **FL4** in the absence of Aβ also accounted for enhancement of the emission intensity relative to that of **FL4** only (Fig. 2). These results indicate that depending on metal ions (Cu^{2+} or Zn^{2+}), **FL4** could be able to chelate metal ions from metal-bound Aβ species to different extents.

Although **FL1** – **FL4** contain the similar core structure to the known compound myricetin[28] and have metal chelation ability described above, they were unable to exhibit an obvious effect on regulating metal-induced Aβ aggregation (Figs. S4 and S5). In the inhibition study, Aβ (10 μM), $CuCl_2$ or $ZnCl_2$ (10 μM), and the ligand (20 μM) were incubated for 24 h at 37 °C with constant agitation. After this time, no significant differences in the distribution of Aβ species visualized by native gel electrophoresis with Western blotting (6E10) were observed for either the metal-free or metal-treated samples suggesting that these ligands did not prevent Aβ aggregation (Fig. S4). To explore whether the ligands might be more suitable to disassemble preformed metal-Aβ aggregates, the disaggregation experiment employing the more soluble compound **FL4** was conducted (Fig. S5). Upon 24 h treatment of **FL4** (50 μM) with preformed Aβ aggregates (25 μM) in the absence or presence of metal ions (25 μM), as with the inhibition study, almost no changes were observed, which indicated that **FL4** was not able to break apart the aggregated Aβ. Possibly, the weak interaction between **FL4** and the peptide (*vide supra*) could be attributed to the limited ability of **FL1** – **FL4** to regulate metal-mediated Aβ aggregation *in vitro*, despite their metal chelation properties. This overall observation suggests that metal chelation alone is insufficient for these molecules to interfere with metal-induced Aβ aggregation and it is paramount to construct structural scaffolds with various functionalities that would lead to appropriate affinities for both metal ions and Aβ species, which could help find suitable chemical tools toward targeting and modulating metal-Aβ species.

The interaction of redox active metal ions with Aβ can generate ROS, which could cause the oxidative stress leading to the development of AD.[1–4,8–11,44,57–59] Metal chelating agents may inhibit ROS production by disrupting metal-Aβ interaction. To investigate the capability of **FL1** – **FL4** in regulating ROS generation by Cu-Aβ species, a horseradish peroxidase (HRP)/Amplex Red assay was employed to monitor the amount of hydrogen peroxide (H_2O_2) in the samples containing of Cu^{2+}, Aβ, and ascorbate in the absence and presence of ligands.[24,25,27] As presented in Fig. 8, **FL3** and **FL4** were able to diminish the production of H_2O_2 by *ca.* 60% and 40%, respectively, which was to a slightly greater degree than myricetin (H_2O_2 generation lowered by *ca.* 30%). These results may suggest that a combination of mechanisms could be at play for flavonoid derivatives in the regulation of ROS, including antioxidant activity, such as that demonstrated for **FL3**, and/or the ability of these molecules to complete for metal binding with the peptides. Particularly, for **FL4**, the latter mechanism may be important since its affinity for Cu^{2+} is within the range of that for Aβ.

Conclusion

Prompted by a need to develop chemical tools to interrogate the role of metal ions associated with Aβ species in AD, four flavonoid derivatives (**FL1** – **FL4**) were chosen on the basis of elements of known flavonoid structures previously reported to be beneficial for metal chelation and Aβ interaction (bifunctionality) and/or regulation of metal-Aβ aggregation and neurotoxicity.[28,37,38] Structural features, including different metal binding moieties and the presence or absence of a dimethylamino group, were considered as a strategy to exploit potential bifunctionality in these compounds. In order to understand how to integrate these molecules into a structure-interaction-reactivity relationship, their properties, such as metal chelation, Aβ interaction, and antioxidant ability, as well as their reactivity toward metal-Aβ species including the ability to regulate metal-induced Aβ aggregation and ROS production were investigated. Although **FL1** – **FL3** were able to chelate metal ions, a limitation for these molecules was their solubility in aqueous buffered solutions. **FL4** was most compatible with aqueous conditions, allowing for more detailed investigations of its metal binding and Aβ interaction properties. From the determination of the solution speciation of **FL4** and its metal complexes, an affinity range for Cu^{2+} and Zn^{2+} ions (nM and μM, respectively) was indicated, such that it might be possible for this ligand to compete with Aβ for metal binding. On the other hand, the direct interaction between **FL4** and Aβ monomer was weak, which was monitored by NMR and MS. Taken with aggregation studies conducted in the presence of metal ions and **FL1** – **FL4**, neither metal chelation nor Aβ interaction was optimized enough to control metal-mediated Aβ aggregation. Furthermore, the addition of the dimethylamino group into the structure alone may also be insufficient to ensure the regulation of Aβ aggregation. Investigations of the antioxidant ability of these flavonoid compounds and their capability to attenuate ROS production have demonstrated that additional beneficial activities of naturally occurring flavonoids could be retained, but some structural refinements to the present compounds might be required to ameliorate this property. Although all four molecules were selected based on expected bifunctionality, they would be more appropriately classified as regular metal chelating agents based on these observations. This present work demonstrates that metal chelation alone is sometimes unable

to sufficiently interrupt the association of metal ions with Aβ species to the degree of some previously known bifunctional small molecules. Thus, comprehensive structure-interaction-reactivity studies employing naturally occurring molecules would be beneficial to obtain suitable structural scaffolds and propose further modifications that may be required to impart reactivity (*e.g.*, metal chelation, Aβ interaction, ROS-scavenging activity). Overall, our studies demonstrate the importance of considering the chemical properties of small molecules so that amendments can be made to finely tune the affinity for Aβ and metal ions (bifunctionality) to specifically interact with and modulate metal-Aβ species.

Supplementary Material

Refer to Web version on PubMed Central for supplementary material.

Acknowledgments

This work is supported by startup funding from the University of Michigan, the Alzheimer's Art Quilt Initiative (AAQI), as well as the Alzheimer's Association (NIRG-10-172326) (to M. H. Lim). B. T. Ruotolo and S.-J. Hyung acknowledge support from the National Institutes of Health (1-R01-GM-095832-01 to B. T. Ruotolo) and the University of Michigan. C. Kim thanks the Korean Science and Engineering Foundation (2009-0074066) for the support. A. S. DeToma acknowledges the National Science Foundation for the Graduate Research Fellowship.

References

1. Jakob-Roetne R, Jacobsen H. Angew Chem Int Ed. 2009; 48:3030–3059.
2. Scott LE, Orvig C. Chem Rev. 2009; 109:4885–4910. [PubMed: 19637926]
3. Rauk A. Chem Soc Rev. 2009; 38:2698–2715. [PubMed: 19690748]
4. (a) DeToma AS, Salamekh S, Ramamoorthy A, Lim MH. Chem Soc Rev. 2012; 41:608–621. [PubMed: 21818468] (b) Pithadia AS, Lim MH. Curr Opin Chem Biol. 2012; in press. doi: 10.1016/j.cbpa.2012.01.016
5. Hardy J, Selkoe DJ. Science. 2002; 297:353–356. [PubMed: 12130773]
6. Frederickson CJ, Koh JY, Bush AI. Nat Rev Neurosci. 2005; 6:449–462. [PubMed: 15891778]
7. Lovell MA, Robertson JD, Teesdale WJ, Campbell JL, Markesbery WR. J Neurol Sci. 1998; 158:47–52. [PubMed: 9667777]
8. Faller P, Hureau C. Dalton Trans. 2009:1080–1094. [PubMed: 19322475]
9. Faller P. ChemBioChem. 2009; 10:2837–2845. [PubMed: 19877000]
10. Tõugu V, Tiiman A, Palumaa P. Metallomics. 2011; 3:250–261. [PubMed: 21359283]
11. Bonda DJ, Lee H-g, Blair JA, Zhu X, Perry G, Smith MA. Metallomics. 2011; 3:267–270. [PubMed: 21298161]
12. Gaggelli E, Kozlowski H, Valensin D, Valensin G. Chem Rev. 2006; 106:1995–2044. [PubMed: 16771441]
13. Bush AI, Tanzi RE. Neurotherapeutics. 2008; 5:421–432. [PubMed: 18625454]
14. Braymer JJ, DeToma AS, Choi JS, Ko KS, Lim MH. Int J Alzheimers Dis. 2011; 2011:623051. [PubMed: 21197068]
15. Cherny RA, Atwood CS, Xilinas ME, Gray DN, Jones WD, McLean CA, Barnham KJ, Volitakis I, Fraser FW, Kim YS, Huang X, Goldstein LE, Moir RD, Lim JT, Beyreuther K, Zheng H, Tanzi RE, Masters CL, Bush AI. Neuron. 2001; 30:665–676. [PubMed: 11430801]
16. Adlard PA, Cherny RA, Finkelstein DI, Gautier E, Robb E, Cortes M, Volitakis I, Liu X, Smith JP, Perez K, Laughton K, Li QX, Charman SA, Nicolazzo JA, Wilkins S, Deleva K, Lynch T, Kok G, Ritchie CW, Tanzi RE, Cappai R, Masters CL, Barnham KJ, Bush AI. Neuron. 2008; 59:43–55. [PubMed: 18614028]

17. Faux NG, Ritchie CW, Gunn A, Rembach A, Tsatsanis A, Bedo J, Harrison J, Lannfelt L, Blennow K, Zetterberg H, Ingelsson M, Masters CL, Tanzi RE, Cummings JL, Herd CM, Bush AI. J Alzheimers Dis. 2010; 20:509–516. [PubMed: 20164561]
18. Crouch PJ, Savva MS, Hung LW, Donnelly PS, Mot AI, Parker SJ, Greenough MA, Volitakis I, Adlard PA, Cherny RA, Masters CL, Bush AI, Barnham KJ, White AR. J Neurochem. 2011; 119:220–230. [PubMed: 21797865]
19. Perez LR, Franz KJ. Dalton Trans. 2010; 39:2177–2187. [PubMed: 20162187]
20. Dedeoglu A, Cormier K, Payton S, Tseitlin KA, Kremsky JN, Lai L, Li X, Moir RD, Tanzi RE, Bush AI, Kowall NW, Rogers JT, Huang X. Exp Gerontol. 2004; 39:1641–1649. [PubMed: 15582280]
21. Wu, W-h; Lei, P.; Liu, Q.; Hu, J.; Gunn, AP.; Chen, M-s; Rui, Y-f; Su, X-y; Xie, Z-p; Zhao, Y-F.; Bush, AI.; Li, Y-m. J Biol Chem. 2008; 283:31657–31664. [PubMed: 18728006]
22. Zhang Y, Chen LY, Yin WX, Yin J, Zhang SB, Liu CL. Dalton Trans. 2011; 40:4830–4833. [PubMed: 21437337]
23. Rodríguez-Rodríguez C, Sánchez de Groot N, Rimola A, Álvarez-Larena Á, Lloveras V, Vidal-Gancedo J, Ventura S, Vendrell J, Sodupe M, González-Duarte P. J Am Chem Soc. 2009; 131:1436–1451. [PubMed: 19133767]
24. Hindo SS, Mancino AM, Braymer JJ, Liu Y, Vivekanandan S, Ramamoorthy A, Lim MH. J Am Chem Soc. 2009; 131:16663–16665. [PubMed: 19877631]
25. Choi JS, Braymer JJ, Nanga RPR, Ramamoorthy A, Lim MH. Proc Natl Acad Sci U S A. 2010; 107:21990–21995. [PubMed: 21131570]
26. Choi JS, Braymer JJ, Park SK, Mustafa S, Chae J, Lim MH. Metallomics. 2011; 3:284–291. [PubMed: 21210061]
27. Braymer JJ, Choi JS, DeToma AS, Wang C, Nam K, Kampf JW, Ramamoorthy A, Lim MH. Inorg Chem. 2011; 50:10724–10734. [PubMed: 21954910]
28. DeToma AS, Choi JS, Braymer JJ, Lim MH. ChemBioChem. 2011; 12:1198–1201. [PubMed: 21538759]
29. Scott LE, Telpoukhovskaia M, Rodríguez-Rodríguez C, Merkel M, Bowen ML, Page BDG, Green DE, Storr T, Thomas F, Allen DD, Lockman PR, Patrick BO, Adam MJ, Orvig C. Chem Sci. 2011; 2:642–648.
30. Hollman PCH, Katan MB. Food Chem Toxicol. 1999; 37:937–942. [PubMed: 10541448]
31. Kim J, Lee HJ, Lee KW. J Neurochem. 2010; 112:1415–1430. [PubMed: 20050972]
32. Ono K, Yoshiike Y, Takashima A, Hasegawa K, Naiki H, Yamada M. J Neurochem. 2003; 87:172–181. [PubMed: 12969264]
33. Hirohata M, Hasegawa K, Tsutsumi-Yasuhara S, Ohhashi Y, Ookoshi T, Ono K, Yamada M, Naiki H. Biochemistry. 2007; 46:1888–1899. [PubMed: 17253770]
34. Porat Y, Abramowitz A, Gazit E. Chem Biol Drug Des. 2006; 67:27–37. [PubMed: 16492146]
35. Mira L, Fernandez MT, Santos M, Rocha R, Florêncio MH, Jennings KR. Free Radical Res. 2002; 36:1199–1208. [PubMed: 12592672]
36. Cao S, Jiang X, Chen J. J Inorg Biochem. 2010; 104:146–152. [PubMed: 19932510]
37. Ono M, Yoshida N, Ishibashi K, Haratake M, Arano Y, Mori H, Nakayama M. J Med Chem. 2005; 48:7253–7260. [PubMed: 16279784]
38. Ono M, Watanabe R, Kawashima H, Kawai T, Watanabe H, Haratake M, Saji H, Nakayama M. Bioorg Med Chem. 2009; 17:2069–2076. [PubMed: 19201614]
39. Leuma Yona R, Mazères S, Faller P, Gras E. ChemMedChem. 2008; 3:63–66. [PubMed: 17926318]
40. Matsugi M, Takeda M, Takahashi A, Tazaki T, Tamura H, Shioiri T. Chem Pharm Bull. 2010; 58:1107–1110. [PubMed: 20686270]
41. Swinney TC, Kelley DF. J Chem Phys. 1993; 99:211–221.
42. Chen CL, Lin CW, Hsieh CC, Lai CH, Lee GH, Wang CC, Chou PT. J Phys Chem A. 2009; 113:205–214. [PubMed: 19072622]
43. Deraeve C, Pitie M, Meunier B. J Inorg Biochem. 2006; 100:2117–2126. [PubMed: 17011628]

44. Himes RA, Park GY, Siluvai GS, Blackburn NJ, Karlin KD. Angew Chem Int Ed. 2008; 47:9084–9087.
45. Gans P, Sabatini A, Vacca A. Ann Chim. 1999; 89:45–49.
46. Alderighi L, Gans P, Ienco A, Peters D, Sabatini A, Vacca A. Coord Chem Rev. 1999; 184:311–318.
47. Jarvet J, Danielsson J, Damberg P, Oleszczuk M, Gräslund A. J Biomol NMR. 2007; 39:63–72. [PubMed: 17657567]
48. Grzesiek S, Bax A, Clore GM, Gronenborn AM, Hu JS, Kaufman J, Palmer I, Stahl SJ, Wingfield PT. Nat Struct Biol. 1996; 3:340–345. [PubMed: 8599760]
49. Garrett DS, Seok YJ, Peterkofsky A, Clore GM, Gronenborn AM. Biochemistry. 1997; 36:4393–4398. [PubMed: 9109646]
50. Foster MP, Wuttke DS, Clemens KR, Jahnke W, Radhakrishnan I, Tennant L, Reymond M, Chung J, Wright PE. J Biomol NMR. 1998; 12:51–71. [PubMed: 9729788]
51. Re R, Pellegrini N, Proteggente A, Pannala A, Yang M, Rice-Evans C. Free Radical Biol Med. 1999; 26:1231–1237. [PubMed: 10381194]
52. Schugar H, Green DE, Bowen ML, Scott LE, Storr T, Böhmerle K, Thomas F, Allen DD, Lockman PR, Merkel M, Thompson KH, Orvig C. Angew Chem Int Ed. 2007; 46:1716–1718.
53. Lipinski CA, Lombardo F, Dominy BW, Feeney PJ. Adv Drug Delivery Rev. 2001; 46:3–26.
54. Clark DE, Pickett SD. Drug Discov Today. 2000; 5:49–58. [PubMed: 10652455]
55. Coles M, Bicknell W, Watson AA, Fairlie DP, Craik DJ. Biochemistry. 1998; 37:11064–11077. [PubMed: 9693002]
56. Rice-Evans CA, Miller NJ, Paganga G. Free Radical Biol Med. 1996; 20:933–956. [PubMed: 8743980]
57. Hureau C, Faller P. Biochimie. 2009; 91:1212–1217. [PubMed: 19332103]
58. Opazo C, Huang X, Cherny RA, Moir RD, Roher AE, White AR, Cappai R, Masters CL, Tanzi RE, Inestrosa NC, Bush AI. J Biol Chem. 2002; 277:40302–40308. [PubMed: 12192006]
59. Shearer J, Callan PE, Tran T, Szalai VA. Chem Commun. 2010; 46:9137–9139.

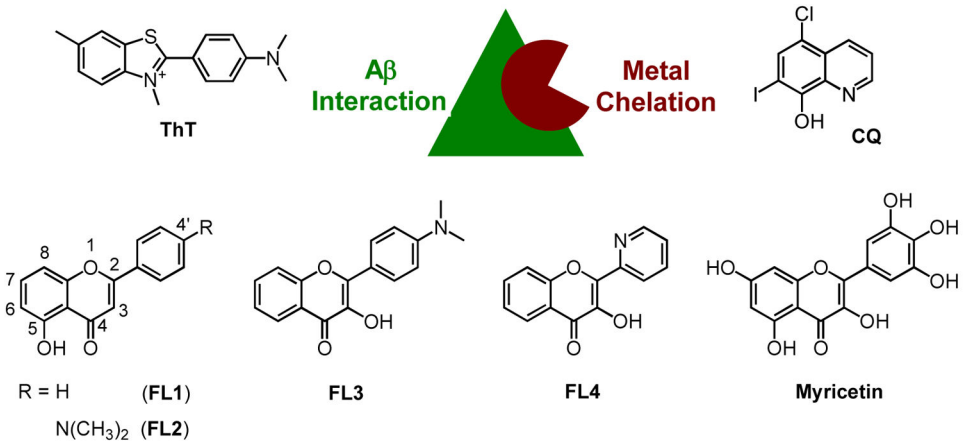

Fig. 1.

Top: Rational structure-based design strategy (incorporation approach: direct inclusion of a metal binding site into an Aβ interacting framework) for the design of bifunctional small molecules. An Aβ interacting structure, thioflavin-T (ThT) (left), and a metal chelating agent, clioquinol (CQ) (right), are depicted. Bottom: Structures of selected flavonoid compounds (**FL1** – **FL4** and myricetin).

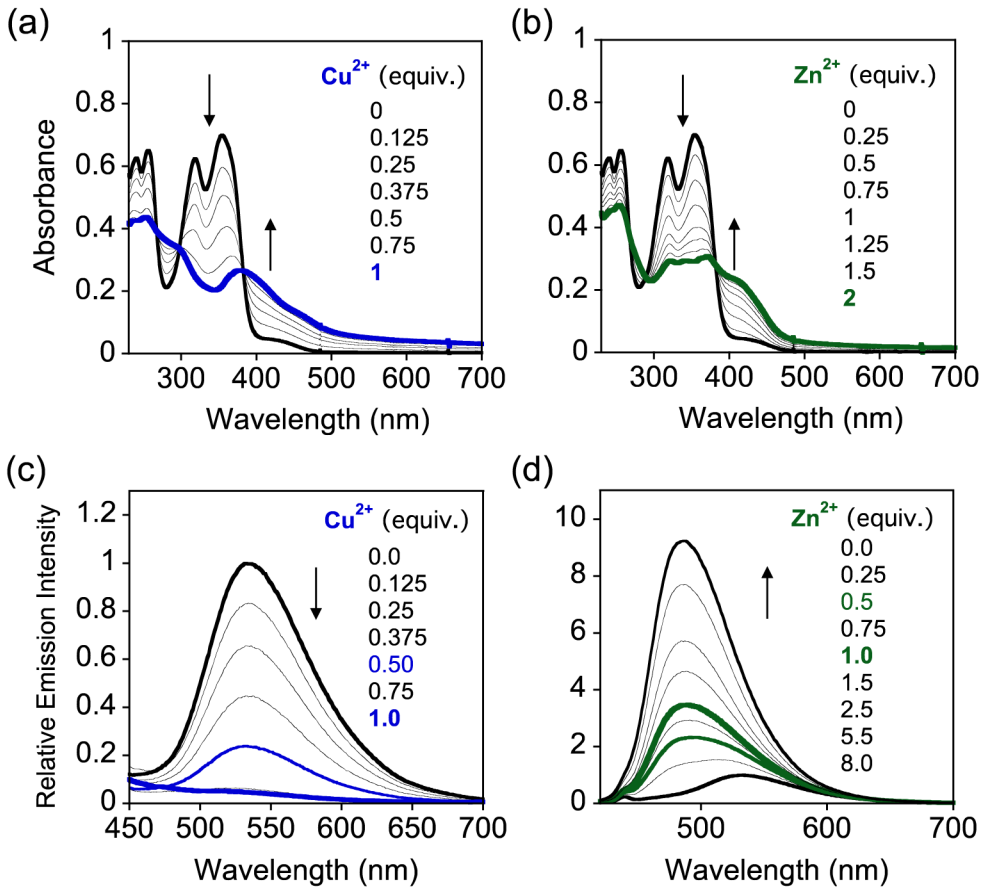

Fig. 2.

Absorption (a, b) and emission spectra (c, d) of **FL4** upon addition of $CuCl_2$ or $ZnCl_2$ at room temperature (20 mM HEPES, pH 7.4, 150 mM NaCl). Experimental conditions: [**FL4**] = 50 μM and 25 μM for UV-Vis and emission (λ_{ex} = 383 nm) measurements, respectively.

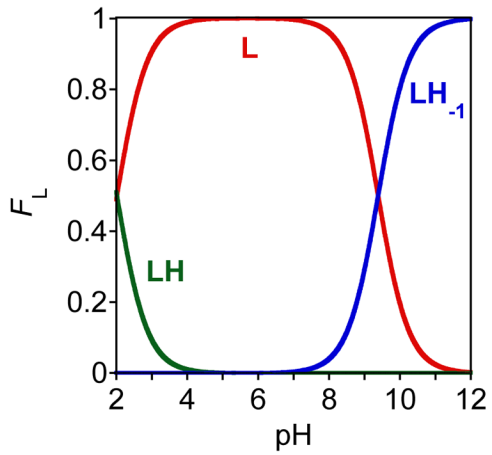

						pK_a [a]
HL	⇌	L	+	H	(pK_{a1})	2.011(8)
L	⇌	LH_{-1}	+	H	(pK_{a2})	9.3892(3)

Fig. 3.

Speciation diagram (top) and acidity constants (pK_a; bottom) of **FL4** (L). Experimental condition: [L] = 50 μM, room temperature, I = 0.10 M NaCl. Charges are omitted for clarity. [a] Error of the last digit is shown in the parentheses.

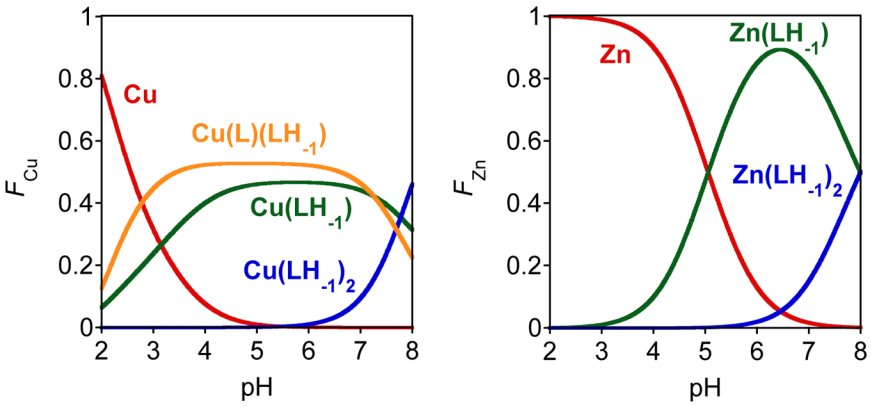

			log β^a	
			Cu^{2+}	Zn^{2+}
$M + LH_{-1}$	⇌	$M(LH_{-1})$	10.97(1)	8.457(2)
$M + L + LH_{-1}$	⇌	$M(L)(LH_{-1})$	17.65(2)	–[b]
$M + 2LH_{-1}$	⇌	$M(LH_{-1})_2$	25.35(2)	14.165(6)

Fig. 4.

Top: Speciation diagrams for **FL4** with Cu^{2+} (left) and Zn^{2+} (right) (pH 2.0 to 8.0). Bottom: Stability constants of Cu^{2+} and Zn^{2+} complexes with **FL4**. Experimental conditions: [M]/[L] = 1:2, $[Cu^{2+}]_{total}$ = 25 μM (90 min incubation with the ligand (L), L = **FL4**), $[Zn^{2+}]_{total}$ = 50 μM (60 min incubation with L), room temperature, I = 0.10 M NaCl. Charges are omitted for clarity. [a] Error of the last digit is shown in the parentheses. [b] The species $Zn(L)(LH_{-1})$ was incorporated to obtain a good fit to the data in the model; a negligible amount was indicated in solution speciation.

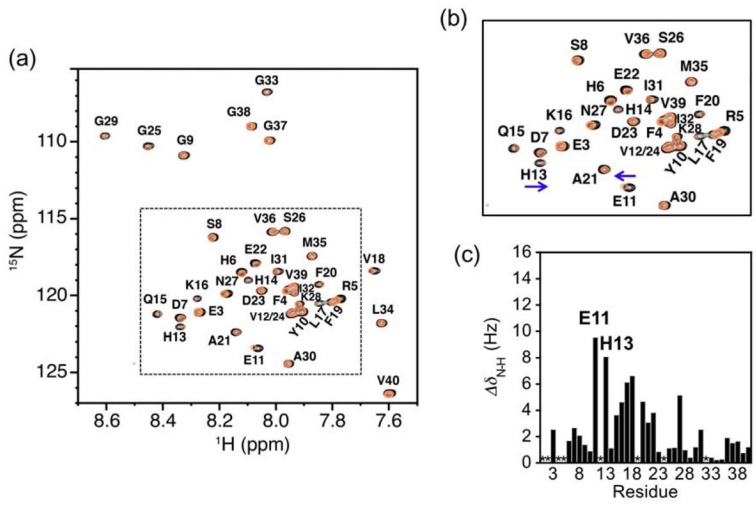

Fig. 5.

Interaction of **FL4** with monomeric $A\beta_{1\text{-}40}$ by 2D ^{1}H–^{15}N TROSY-HSQC NMR spectroscopy. (a) Spectra of the ^{15}N-labeled Aβ peptide (black, 200 mM SDS-d_{25}, 20 mM sodium phosphate, 7% D_2O (v/v), pH 7.3, 25 °C) followed by the addition of 20 (orange) equivalents of **FL4**. The dotted box indicates the expanded view shown in (b) displaying the residues most significantly affected by the presence of **FL4**. (c) Plot of the change in chemical shift ($\Delta\delta_{N-H}$) as a function of the peptide sequence upon the addition of 20 equivalents of **FL4**. * Denotes absent or overlapping peaks. The values of $\Delta\delta_{N-H}$ were calculated using equation (1).

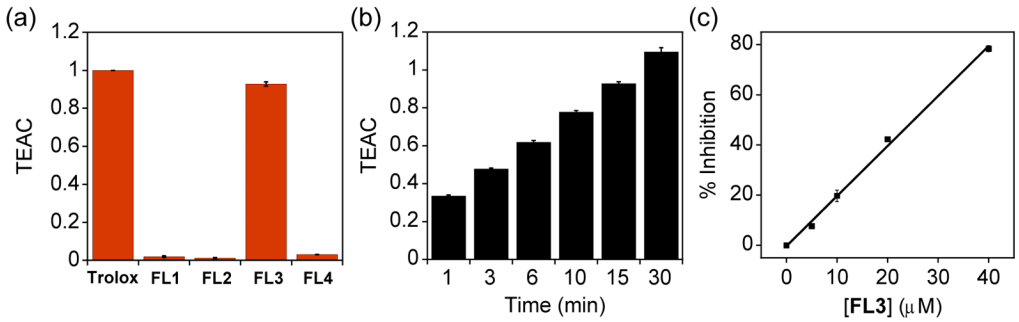

Fig. 6.

Trolox equivalent antioxidant capacity (TEAC) values of (a) Trolox and **FL1** – **FL4** (15 min incubation) and of (b) **FL3** for 1, 3, 6, 10, 15, and 30 min incubation. (c) The effect of [**FL3**] on the inhibition of the $ABTS^{\cdot+}$ (15 min incubation).

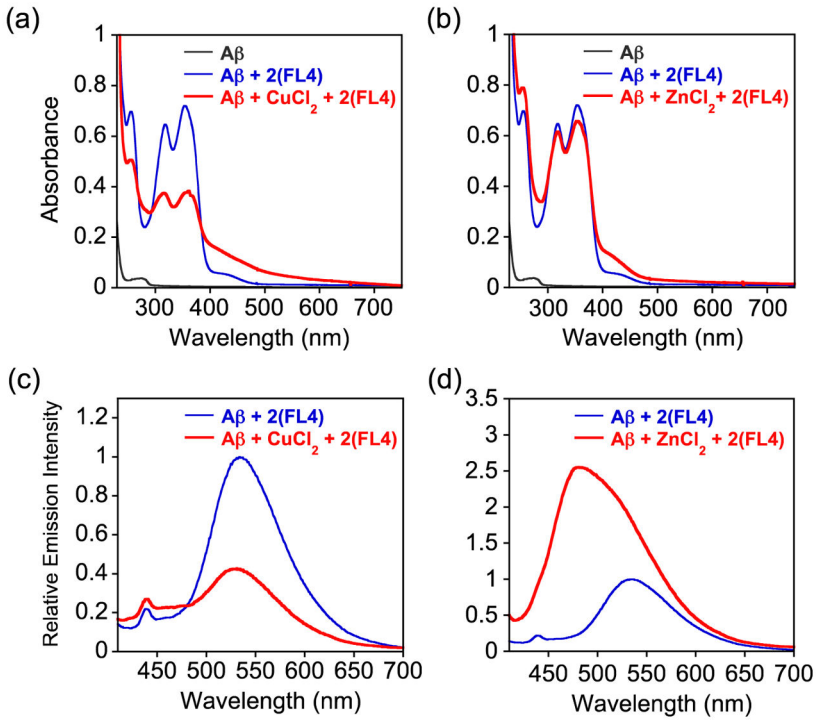

Fig. 7.

Absorbance (a, b) and emission (c, d) spectra showing the interaction of **FL4** with metal ions in the presence of Aβ at room temperature. The spectra of **FL4** and Aβ in the absence and presence of metal ions are shown in blue and red, respectively. To Aβ, $CuCl_2$ or $ZnCl_2$ was added and incubated for 2 min followed by the treatment with **FL4** for 5 min (red). Experimental conditions: [Aβ] = 25 μM, [$CuCl_2$ or $ZnCl_2$] = 25 μM, [**FL4**] = 50 μM, 20 mM HEPES, pH 7.4, 150 mM NaCl.

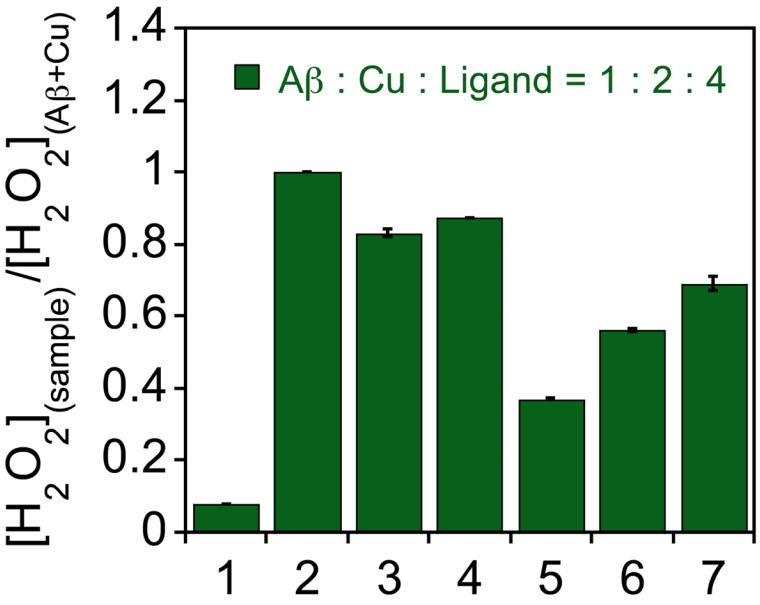

Fig. 8.

Detection of H_2O_2 from samples of Aβ, Cu^{2+}, and/or a compound in the presence of ascorbate by a horseradish peroxidase (HRP)/Amplex Red assay. Lanes: (1) Aβ; (2) Aβ + Cu^{2+}; (3) Aβ + Cu^{2+} + **FL1**; (4) Aβ + Cu^{2+} + **FL2**; (5) Aβ + Cu^{2+} + **FL3**; (6) Aβ + Cu^{2+} + **FL4** ; (7) Aβ + Cu^{2+} + myricetin. Experimental conditions: [Aβ] = 200 nM, [Cu^{2+}] = 400 nM, [ligand] = 800 nM, [ascorbate] = 10 μM, [Amplex Red] = 50 μM, [HRP] = 1 U/mL, $\lambda_{ex/em}$ = 530/590 nm. Catalase attenuates the fluorescence signal.